6th European Conference on Computational Mechanics (ECCM 6)
7th European Conference on Computational Fluid Dynamics (ECFD 7)
1115 June 2018, Glasgow, UK

FAST COMPUTATION OF A SMOOTH YARN'S VELOCITY IN A MAIN NOZZLE

LUCAS DELCOUR[1], JOZEF PEETERS[2], JORIS DEGROOTE[1,3] AND JAN VIERENDEELS[1,3]

[1]Ghent University, Faculty of Engineering and Architecture, Department of Flow, Heat and Combustion Mechanics, Sint-Pietersnieuwstraat 41, B-9000 Ghent Belgium, https://www.ugent.be/ea/floheacom/en, lucas.delcour@ugent.be

[2]Picanol NV, Steverlyncklaan 15, 8900 Ieper Belgium, http://www.picanol.be/en, info@picanol.be

[3]Flanders Make, Belgium

Key words: Computational fluid dynamics, Air jet loom, Main nozzle, Fluid-structure interaction

Abstract. Air jet weaving looms are well-known for their high insertion rates. The attainable insertion rate is directly dependent on the yarn velocity, which is mainly imposed by the main nozzle. The complex flow patterns arising in those nozzles make it difficult to predict how a change in geometry or supply pressure will affect the yarn velocity.

In this paper a computational fluid dynamics (CFD) model is coupled with a simplified structural model to calculate the axial velocity of a smooth yarn as it is launched by the main nozzle without using experimentally determined force coefficients. Instead, the force on the yarn is calculated by integrating the wall shear stress, obtained using a RANS model, on a no-slip wall representing the yarn. The results are compared to experiments in which the yarn velocity is obtained from high speed footage. By using a smooth yarn the influence of yarn hairiness is omitted and uncertainty on the yarn diameter is reduced.

In the flow model the yarn is modeled as a rigid cylinder centered on the axis, allowed to move in the axial direction by a moving wall boundary condition. In the structural model the inertial force corresponding to the acceleration of a stationary piece of yarn to the current yarn velocity, the inertial force associated to an increase or decrease of the yarn velocity and the force exerted by the air flow on the yarn (obtained from the flow simulation) are considered. Calculations are performed on a single nozzle geometry and the sensitivity with respect to simplifications and numerical parameters is investigated.

From the results, it can be concluded that a reasonable estimate for the velocity of a smooth yarn can be obtained without force coefficients and with relatively limited computational resources. The shocks appearing inside the main nozzle do not have to be accurately resolved if one is only interested in the axial motion of the yarn. The acceleration of the yarn tends to take longer in the simulations compared to the experiments. This is most likely caused by the fact that the yarn is considered inelastic in the simulations and that the yarn is not stretched at the start of the experiment.

1 INTRODUCTION

In air-jet weaving looms, the main nozzle is supplied with highly pressurized air to generate a high-velocity air flow. This air flow exerts a propulsive force on the yarn, which passes through the main nozzle, launching it into the reed. Due to the complex flow inside the main nozzle and the interaction of the yarn with the flow, improvement of the aerodynamics in these machines is not straightforward and often requires extensive experimental trials. Fluid-structure interaction (FSI) simulations can provide additional insight into the yarn and flow behavior or can be used to evaluate modifications without actually constructing the altered part.

The first attempts at modeling the dynamic yarn behavior inside the main nozzle of an air-jet weaving loom ignored the influence of the yarn on the flow and relied on theoretical, idealized flow patterns or empirically determined formulas for the flow. In 1972, Uno [1] established the equations of motion for a weft yarn, assumed to be inextensible and to move along the axis, which he then solved numerically based on an empirical model for the air velocity distribution. Adanur and Mohamed [2, 3] developed a theoretical model for yarn motion of both drum and loop storage. The yarn was again assumed to be inextensible and to move along the axis of the nozzle. They used an empirical flow model based on measurements of the centerline velocity at different locations. Nosraty et al. [4] constructed and numerically solved the equations of motion for a yarn launched from a single nozzle. They combined models for jet velocity, friction coefficient and yarn structure to best agree with experimental results. Celik and Babaarslan [5] followed a similar approach but, additionally, took into account the presence of the reed, relay nozzles and a stretching nozzle. The force on the yarn was evaluated using multiple time and place dependent empirical formulas.

As computational power increased the use of computational fluid dynamics (CFD) and finite-element modeling (FEM) for evaluation of the dynamic yarn behavior became feasible. De Meulemeester et al. [6] used a 1D finite-element model to calculate the tension in the yarn at the end of insertion for an air-jet weaving loom. Later on the model was extended to 3D [7] to simulate the unwinding of a yarn from a smooth cylinder. Wu et al. [8] used an ALE approach on a 2D, planar geometry to simulate the whipping behavior of a yarn during startup of a weft insertion. FSI simulations with two-way influence were performed without axial motion of the yarn. For simulating the motion of a weft yarn in high-speed flows within confined spaces, the use of an arbitrary Lagrangian-Eulerian (ALE) approach is not straightforward due to the flexibility of the thread and the resulting mesh deformations. Additionally, FSI simulations with two-way influence on 3D geometries require significant amounts of computational power. Therefore, Osman et al. [9] proposed a different procedure: a static mesh is used with a fixed rigid cylinder on the axis and the motion of the yarn is taken into account by adding a source term to the momentum equation. A 2D, axisymmetric fluid model was employed, considerably reducing the required calculation time. For the yarn the structural model from De Meulemeester et al. [7] was slightly adapted to incorporate bending forces. The aerodynamic forces on the yarn were calculated using the local relative velocity of the yarn in combination

with constant longitudinal and normal force coefficients. These force coefficients, which determine the interaction of the yarn with the flow, however, have to be determined empirically. Furthermore, it has been shown that the force coefficient varies substantially with the relative air velocity [1, 10, 11], thus, the use of fixed coefficients is a rather crude assumption. Tabulating the coefficient over the velocity range would require extensive and meticulously executed experiments, especially when considering high-speed compressible flows, as encountered in present-day main nozzles.

In this research a simplified FSI framework is established to calculate the axial velocity of a smooth yarn as it is launched by the main nozzle. It is assumed that the elasticity of the yarn has limited influence on the axial force and is of limited importance for the velocity. This assumption allows the yarn to be modeled as inextensible, avoiding the need of a finite element model for the yarn. Additionally, as smooth yarns are used, there is no need for experimentally obtained force coefficients. The yarn itself is modeled as a rigid cylinder on the axis with a moving wall boundary condition, eliminating the need for a dynamic mesh. As such, the methodology requires only limited computational resources, contrary to full-scale 3D FSI simulations. For validation, the calculations are, without any tuning, compared to experimental measurements.

2 METHODOLOGY

In this research FSI simulations with 2-way influence are performed. When using a Dirichlet-Neumann domain decomposition, this requires a flow model which is able to incorporate the dynamics of the structure and a structural model subjected to the forces exerted by the flow. The structural model is discussed first, as its implementation is of importance to the flow model. After outlining both models the coupling is discussed. The results are compared to experimental measurements obtained from the setup described at the end of this section.

2.1 Structural model

The structural model, representing the yarn, consists of a rigid cylinder, centered on the axis of the nozzle. Only axial motion of the cylinder is allowed, resulting in a single-degree-of-freedom system. As the cylinder represents the yarn in the main nozzle and downstream of it up to a certain distance, the mass of the cylinder increases linearly with the axial displacement. The initial mass corresponds to that of the yarn in between the nozzle exit and the yarn supply (see Figure 1). The experimental setup is designed to minimize yarn ballooning (by careful preparation of the windings) as well as friction in the guide eye (by using a polymer lining). These forces are, thus, not considered in the model. The three dominant forces are included: the aerodynamic force, exerted by the flow on the yarn, the yarn withdrawal force, corresponding to the acceleration of a new section of yarn to the instantaneous velocity and the force to change the speed of the yarn.

The aerodynamic force is obtained from the flow model and will be discussed later on. The yarn withdrawal force (T) originates from a piece of yarn, located in the storage

device, which has to be accelerated from zero velocity to the yarn velocity at that instant. An expression for this force can be derived from a momentum balance. If the yarn is moving at a uniform velocity u_d and accelerates a stationary piece of yarn, then the momentum-increase in a time step Δt corresponds to

$$\Delta P = \Delta m \cdot u_d = (\rho_A \cdot u_d \cdot \Delta t) \cdot u_d, \text{ with } \rho_A \text{ the linear mass density of the yarn.} \quad (1)$$

An expression for the yarn withdrawal force can be obtained by taking the limit for infinitesimally small time steps:

$$T = \lim_{\Delta t \to 0} \left(\frac{\Delta P}{\Delta t} \right) = \frac{\mathrm{d}P}{\mathrm{d}t} = \rho_A \cdot u_d^2 \quad (2)$$

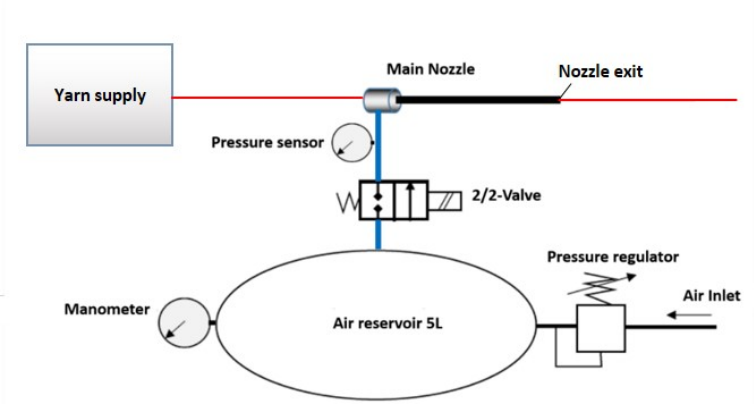

Figure 1: Schematic representation of the experimental setup.

2.2 Flow model

For the compressible flow calculations, a pressure-based solver with the coupled pressure-velocity scheme is used. The k-ω SST model is employed as turbulence model. A first-order implicit time-discretization scheme was chosen, in combination with second-order upwind schemes for the convective terms in the density, momentum and energy equations. At the pressure inlet, a case-specific pressure profile, obtained from experiments, is imposed. The model is 2D-axisymmetric with the yarn represented as a rigid cylinder on the axis. To incorporate the axial yarn motion, a moving wall boundary condition is assigned to the cylinder wall. The velocity is obtained from the coupling between the structural and flow model; this is elaborated on in the next section. Calculations are performed in Fluent 17.2. The flow domain with an indication of the boundary conditions can be found in Figure 2. The domain extends up to 0.5 m downstream of the nozzle. The nozzle itself is about 30 cm long and its exit diameter is 4 mm.

2.3 Coupling

A coupling code was written for the specific cases considered. Since the structural model is not complex, there is no need for a dedicated structural solver. Instead, the

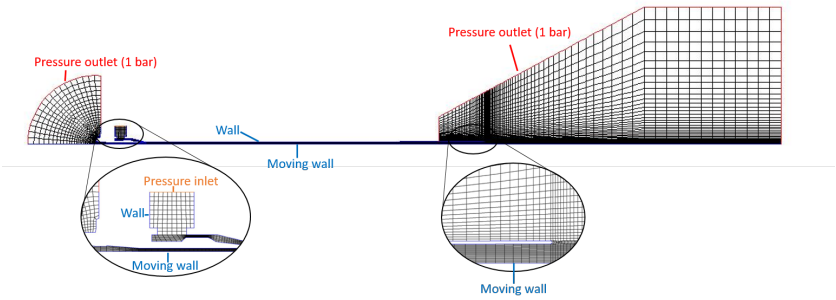

Figure 2: Flow domain with indication of the boundary conditions.

structural calculations are directly included in the coupling code. The fundamental concept is as follows: the flow solver calculates the flow and, from this, the aerodynamic force experienced by the yarn. Subsequently, the structural model uses this force as input and employs Newton's second law to calculate the yarn acceleration. This acceleration is, then, used to calculate the velocity and displacement of the yarn after the current time step. A more detailed explanation on the iterative procedure is given below.

The coupling code is configured to allow for both explicit and implicit FSI coupling. The explicit calculation is discussed first. For the explicit method, the velocity at time $t + \mathrm{d}t$ is obtained from the velocity and acceleration at time t according to the following formula (x = displacement $[m]$, x_d = velocity $[m/s]$, x_{dd} = acceleration $[m/s^2]$):

$$x_d|_{t+\mathrm{d}t} = x_d|_t + x_{dd}|_t \cdot \mathrm{d}t \tag{3}$$

The displacement and mass at time $t + \mathrm{d}t$ follow from:

$$x|_{t+\mathrm{d}t} = x|_t + x_d|_t \cdot \mathrm{d}t + x_{dd}|_t \cdot \frac{\mathrm{d}t^2}{2} \tag{4}$$

$$m|_{t+\mathrm{d}t} = \rho_A \cdot \left(l_0 + min\left(x_{max}, x|_{t+\mathrm{d}t}\right)\right) \tag{5}$$

The value of x_{max} should be set in advance. It is used to specify that from a certain axial distance on, the yarn is no longer subjected to a significant force. Consequently, it is no longer stretched and its mass is then removed from the inertial term used to calculate the acceleration of the yarn according to Newton's second law, see Formula 6. After imposing the obtained wall velocity in the flow solver, the new flow is calculated and the driving force (F) for the yarn is calculated. Subsequently, the acceleration at time $t + \mathrm{d}t$ is retrieved as follows:

$$x_{dd}|_{t+\mathrm{d}t} = \frac{F - \rho_A \cdot x_d^2|_{t+\mathrm{d}t}}{m|_{t+\mathrm{d}t}} \tag{6}$$

The sequence (3) to (6) is repeated until the desired flow time is reached.

The implicit method uses quasi-Newton iterations to reduce the residual at $t+\mathrm{d}t$. The residual (R) is defined as:

$$R|_{t+\mathrm{d}t} = \left\| F|_{t+\mathrm{d}t} - (m \cdot x_{dd})|_{t+\mathrm{d}t} - \rho_A \cdot x_d^2|_{t+\mathrm{d}t} \right\| \tag{7}$$

The first coupling iteration ($k = 1$) is the same as in the explicit method and provides an estimate for the acceleration at $t + \mathrm{d}t$. From the second coupling iteration onward, the velocity at time $t + \mathrm{d}t$ is retrieved via a Crank-Nicholson approach instead of an explicit Euler, see Formula 8.

$$x_d|_{t+\mathrm{d}t} = x_d|_t + \left(x_{dd}|_t + x_{dd}|_{t+\mathrm{d}t}\right) \cdot \frac{\mathrm{d}t}{2} \tag{8}$$

The displacement at time $t + \mathrm{d}t$ follows from:

$$x|_{t+\mathrm{d}t} = x|_t + x_d|_t \cdot \mathrm{d}t + \left(x_{dd}|_t + x_{dd}|_{t+\mathrm{d}t}\right) \cdot \frac{\mathrm{d}t^2}{4} \tag{9}$$

The newly obtained velocity is, then, imposed and the force at $t + \mathrm{d}t$ is retrieved from the flow simulation. This allows the residual to be calculated. The residuals obtained from the first 2 coupling iterations are used to obtain a finite difference approximation for the derivative of the residual with respect to the acceleration at time $t + \mathrm{d}t$. This estimate is used to update the acceleration at time $t + \mathrm{d}t$. The sequence is repeated until the residual drops below a specified threshold. If, after a selected amount of inner iterations, no convergence is reached, the derivative is recalculated. It should also be mentioned that in the flow solver, the force is obtained by integrating over the entire axial length of the domain. This is not entirely consistent since the yarn does not necessarily span the entire domain. To assess the effect this has on the calculations, a separate code was developed which splits the cylinder wall at the physical location of the yarn tip. The driving force is, then, only integrated over the leftmost part.

2.4 Experimental setup

An experimental setup was constructed by Picanol NV (Ieper, Belgium) to validate the calculations. A schematic representation of this setup can be found in Figure 1. The yarn velocity is derived from high speed recordings of the yarn entering the main nozzle. Prior to launch, black markings are applied to the yarn at regular intervals. As was mentioned previously, the setup was designed to minimize yarn ballooning, this is accomplished by carefully storing the windings in a dedicated yarn supply device. Since a smooth surface was desired, a polymer coated yarn was selected. The yarn has an average diameter of 0.72 mm and a linear density of 76 tex (g/km). To obtain more accurate data for the simulations, the yarn that passed through the main nozzle is cut off and weighed to determine the average linear density of that specific section.

The yarn is launched by supplying highly pressurized air to the main nozzle. To this end, an air reservoir with adjustable pressure is connected to the main nozzle through a valve. In this research, reservoir gauge pressures of 3 bar and 5 bar were used. The pressure in front of the main nozzle is recorded and the measured profiles are used as input for the CFD calculations. The measured pressure profiles are displayed in Figure 3.

3 RESULTS

All simulations discussed in this paper are performed on a single nozzle geometry. The nozzle has a conical jet inlet and a conical tube section. Figure 4 shows a sketch with

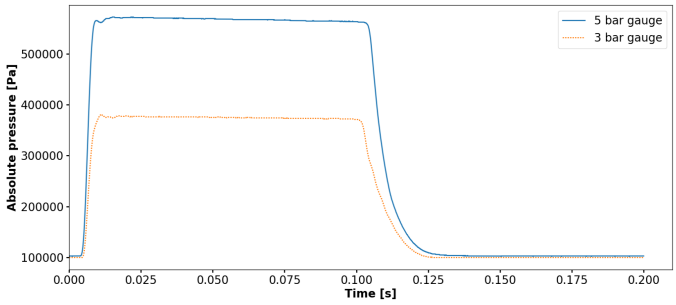

Figure 3: Gauge pressures measured at the nozzle inlet. These profiles are also used as input to the simulations.

exaggerated radial dimensions (top) as well as a contour plot of the velocity magnitude in such a nozzle (bottom). The presence of shocks and supersonic flow can clearly be observed.

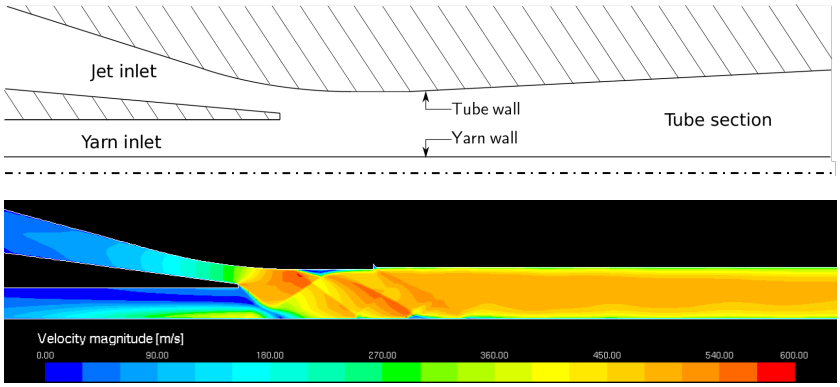

Figure 4: Sketch of the nozzle geometry (top) [not to scale]. Contour plot of velocity magnitude at 5 bar gauge pressure (bottom).

Since transient simulations are performed, initial conditions have to be specified. The initial yarn displacement, velocity and acceleration are set to zero. An initial length, however, has to be specified. This initial length mainly plays a role during the initial acceleration of the yarn. For sensitivity studies, the initial length is chosen rather small ($l_0 = 0.09\ m$) as this allows the yarn to accelerate faster to an equilibrium velocity which reduces the required computational time. By contrast, when the simulations are to be compared to the measurements, the initial length ($l_0 = 0.584\ m$) is chosen equal to the space between the nozzle exit and the yarn supply device (see Figure 1).

As a first step in this paper, the sensitivity of the model with respect to some simplifications and numerical parameters is investigated. To this end calculations at 5 bar gauge pressure are considered as these yield the highest accelerations. Later on a simulation at 3 bar gauge pressure is also performed.

3.1 Need for FSI

To illustrate the need of incorporating the axial motion into the flow simulations, a calculation is performed in which the yarn velocity is computed, but not imposed. The results at 5 bar gauge pressure can be found in Figure 5.

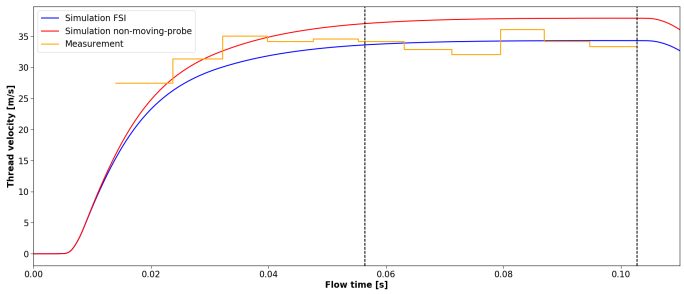

Figure 5: Effect of incorporating the yarn motion into the simulation for $l_0 = 0.584$ m and 5 bar gauge pressure.

As can be seen from the figure, not incorporating the yarn motion in the flow simulation leads to an overestimation of the yarn velocity. Over the indicated interval, the average velocity for the simulation without yarn motion is 37.7 m/s, for the FSI simulation this was 34.2 m/s and the measurement resulted in an average of 33.7 m/s.

3.2 Explicit versus Implicit FSI Coupling

To verify whether it is worth the additional computational effort of performing implicit FSI coupling, a comparison is made between the results of an implicit FSI coupling and an explicit FSI coupling. A gauge pressure of 5 bar is considered and the initial length l_0 is set to 0.09 m. Figure 6 depicts the results as well as the observed difference between both. It can be seen that the difference between both velocity profiles is negligible. The implicit calculation required about 50 hours of computational time while the explicit calculation could be performed within 10 hours on a single core of a 12-core Intel Xeon E5-2680v3 2.5 GHz CPU. Therefore, the choice was made to use the explicit algorithm for the remainder of the calculations.

3.3 Mesh sensitivity

Calculations are performed on a rather coarse mesh with approximately 10 000 cells to limit the required computational time. The y^+ values are well above 30 for the zones of interest, implying that wall functions are used. It should, however, be noted that shocks occur in the nozzle due to the supersonic flow in certain zones. To accurately resolve the shocks and their interaction with the boundary layers, a much higher mesh resolution is required. The influence of the mesh size is investigated by performing simulations on meshes uniformly refined in both x- and y-direction. Meshes with 4 times and 16 times the amount of cells are considered. The velocities are displayed in Figure 7. The largest difference is about 0.4 m/s. Considering the huge increase in cost that comes with running

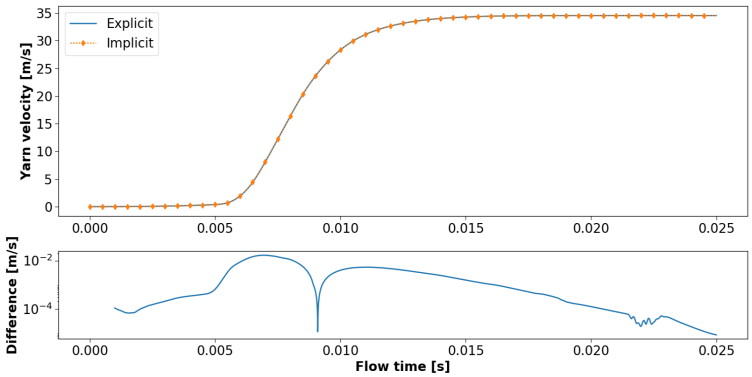

Figure 6: Comparison between implicit and explicit FSI coupling for $l_0 = 0.09$ m and 5 bar gauge pressure. The maximal difference is 0.02 m/s.

simulations with 16 times more cells, the difference is deemed acceptable and calculations are continued on the base mesh with some local refinement, resulting in approximately 11 500 cells.

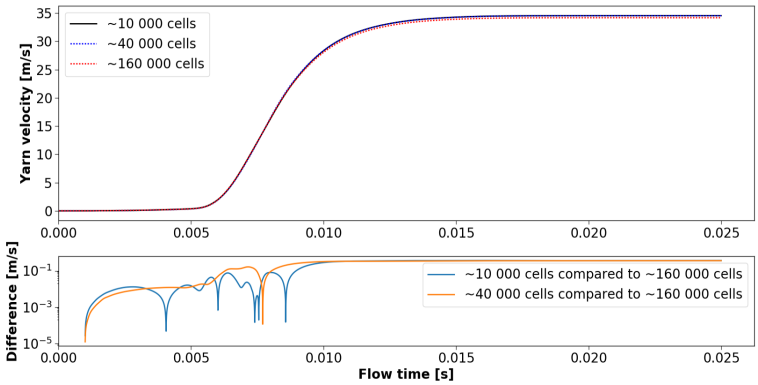

Figure 7: Influence of mesh size on yarn velocity for $l_0 = 0.09$ m and 5 bar gauge pressure. The maximal difference is 0.37 m/s.

3.4 Time step sensitivity

Apart from the mesh size, the choice of time step can also influence the results. Simulations are typically performed using a time step of 5e-6 s. The influence of time step size is investigated by considering time steps of 2.5e-6 s and 1.25e-6 s. The results are depicted in Figure 8. The observed difference in yarn velocity remains quite low and thus, a time step of 5e-6 s is opted for.

3.5 Effect of integrating the wall shear stress over the entire axial length

In the simulations the force on the yarn is obtained by integrating the wall shear stress over a rigid cylinder that extends throughout the entire domain. This domain has to extend quite some distance beyond the nozzle exit, not to hinder the jet development in

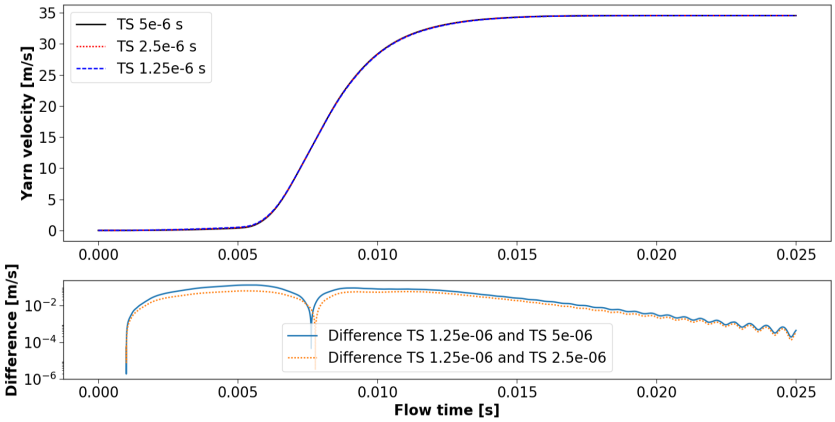

Figure 8: Influence of time step size on velocity for $l_0 = 0.09$ m and 5 bar gauge pressure. The maximal differences are 0.13 m/s and 0.06 m/s.

the flow simulations. Two distinct effects can now come into play. On the one hand the jet needs some time to develop and only has a finite axial influence range. This implies that, from a certain axial distance onward, the yarn velocity exceeds that of the surrounding air, resulting in a braking force on the cylinder. On the other hand it could be that, in reality, the yarn tip has not been propelled as far as the jet has propagated. This can result in an overestimation of the simulated force due to part of the wall shear stress being taken into account over a region where, physically, there is no yarn present. To analyze these effects, a separate piece of code was written which only imposes a velocity to the first part of the cylinder and considers only this part for the force. Initially, the cylinder is split at the nozzle exit and during the simulation the split location is moved along with the calculated yarn displacement. The simulations are performed with an initial length l_0 of 0.584 m at 5 bar gauge pressure. Figure 9 compares both simulations.

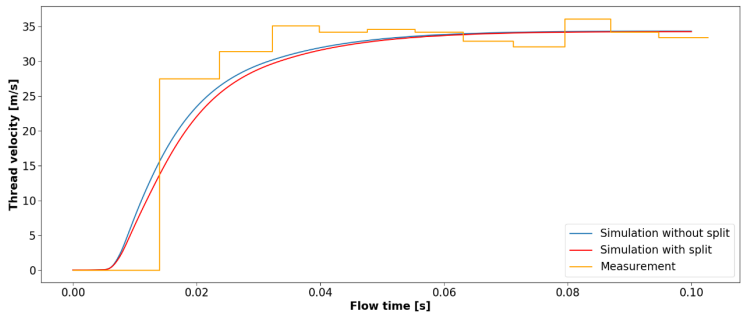

Figure 9: Effect of splitting the cylinder wall at the yarn tip for $l_0 = 0.584$ m and 5 bar gauge pressure.

From Figure 9 it can be seen that splitting the wall slows down the initial acceleration, for the case considered. This implies that the effect of the jet having propagated further than the yarn causes a difference of at most 1.92 m/s during the start. Moreover, for the considered simulations there is almost no braking effect as by the time the yarn

attains a considerable velocity, the surrounding air has attained an even higher velocity. If the domain were to be enlarged considerably, the braking force might gain importance, especially since the jet would then only influence a small axial part of the atmosphere. In the splitting approach the split location has to vary during the calculation. This requires the cylinder walls to be merged and split again at least once per time step. Due to the large number of time steps to be performed, this procedure increases the total simulation time substantially and is, therefore, not used in other calculations.

3.6 Comparison to experiment

Based on the previous observations, simulations are performed at gauge pressures of 3 bar and 5 bar and compared to experimental measurements. The simulations start from zero initial displacement, initial velocity and initial acceleration. An initial length of 0.584 m is imposed. The mesh consists of about 11 500 cells and a time step of 5e-6 s is employed. The simulations are performed without splitting of the cylinder wall at the yarn tip, implying that the yarn velocity is imposed over the entire axial length of the cylinder and the wall shear stress is also integrated over this entire length. An explicit FSI coupling is used. The results of these calculations are shown in Figure 10.

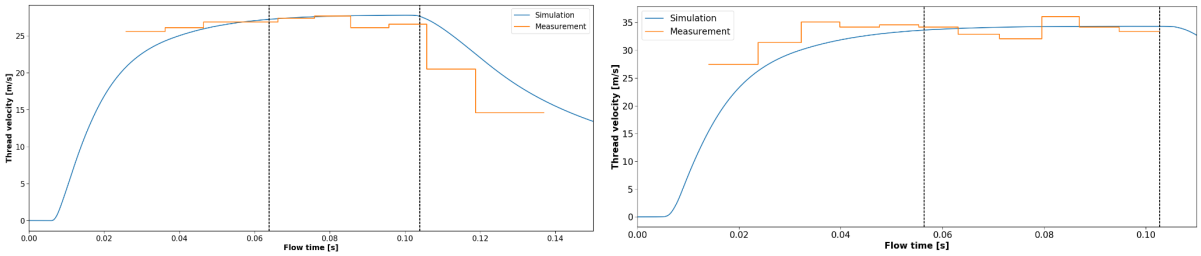

Figure 10: Transient velocity profile for polymer coated yarn launched at 3 bar (left) and 5 bar (right) gauge pressure. Dotted lines indicate the averaging interval.

To compare the regime velocities the velocity profiles are averaged out over a time interval, starting when the simulated velocity reaches 98% of the maximum simulated velocity and ending when the simulated velocity starts decreasing again or at the last measurement point. For 3 bar gauge pressure this results in an average simulated velocity of 27.6 m/s and an average measured velocity of 27.0 m/s. For 5 bar gauge pressure the obtained values are 34.2 m/s for the simulation and 33.7 m/s for the measurements. Note, however, that these calculations have been performed on a rather coarse grid without any tuning to yarn diameter and/or roughness. The deceleration trend of the yarn with 3 bar gauge pressure is also captured quite well, but will not be considered further on as it was not the goal of this research. It can be seen from the figures that the yarn acceleration takes quite long in the simulation compared to the measurements. The slow transient behavior at startup is most likely due to the choice of the initial length (l_0). The simulation methodology implies that the entire length l_0 has to be accelerated as a rigid cylinder, while in reality the yarn has some axial flexibility and is not under tension at start.

4 CONCLUSION

Despite the simple structural model and the applied simplifications, the current model is capable of providing a good estimate of the yarn velocity for a smooth yarn without the use of force coefficients or additional tuning. The initial acceleration of the yarn in the simulations is, however, quite slow compared to the experiments. This is most likely due to the fact that in the simulations the yarn is considered as a rigid cylinder while in reality the yarn has some elasticity. Furthermore, the yarn was not tensioned at the start of the experiment.

REFERENCES

[1] Uno, M. A Study on Air-Jet Loom with Substreams Added. *Journal of the textile machinery Society of Japan* (1972) **25**:48–56

[2] Adanur, S. and Mohamed, M.H. Analysis of yarn tension in air-jet filling insertion. *Textile Research Journal* (1991) **61**:259–266

[3] Adanur, S. and Mohamed, M.H. Analysis of yarn motion in single-nozzle air-jet filling insertion. *The Journal of the Textile Institute* (1992) **83**:45–55

[4] Nosraty, H. Jedi, A.A.A. Mousaloo, Y. Simulation analysis of weft yarn motion in single nozzle air-jet loom to study the effective parameters. *Indian Journal of Fibre & Textile Research* (2008) **33**:45–51

[5] Celik, N. and Babaarslan, O. A mathematical model for numerical simulation of weft insertion on air-jet weaving machine. *Textile Research Journal* (2004) **74**:236–240

[6] De Meulemeester, S. Githaiga, J. Van Langenhove, L. and Hung, D.V. Simulation of the dynamic yarn behavior on airjet looms. *Textile Research Journal* (2005) **75**:724–730

[7] De Meulemeester, S. Puissant, P. and Van Langenhove, L. Three-dimensional simulation of the dynamic yarn behavior on Air-jet Looms. *Textile Research Journal* (2009) **79**:1706–1714

[8] Wu, Z. Chen, S. Liu, Y. and Hu, X. Air-flow characteristics and yarn whipping during start-up stage of air-jet weft insertion. *Textile Research Journal*(2016) **86**:1988–1999

[9] Osman, A. Malengier, B. De Meulenmeester, S. Peeters, J. Degroote, J. and Vierendeels, J. Simulation of air flow-yarn interaction inside the main nozzle of an air jet loom. *Textile Research Journal*(2017) **0**:1–11. DOI:10.1177/0040517517697646

[10] Anderson, S. L. and Stubbs, R. Use of air currents for tensioning fibres. *Journal of the Textile Institute Transactions*(1958) **49**:53–57

[11] Selwood, A. The Axial air-drag of Monofilaments. *Journal of the Textile Institute Transactions*(1962) **53**:576